ARTICLE
Journal of Cellular Biochemistry 116:533–541 (2015)

Journal of Cellular Biochemistry

Epigenetic Modifications, Chromatin Distribution and *TP53* Transcription in a Model of Breast Cancer Progression

Gilson C. Santos Jr,[1,2] Ana P. A. da Silva,[1] Lucas Feldman,[1] Grasiella M. Ventura,[3] Yegor Vassetzky,[2] and Claudia V. de Moura Gallo[1]*

[1]*Departamento de Genética, Instituto de Biologia Roberto Alcantara Gomes, Universidade do Estado do Rio de Janeiro, Rio de Janeiro 20550-013, Brazil*

[2]*Université Paris-Sud 11 CNRS UMR 8126 «Signalisation, Noyaux et Innovations en Cancérologie», Institut de Cancérologie Gustave-Roussy, Université Paris-Sud 11, F-94805, Villejuif Cedex, France*

[3]*Instituto de Ciências Biológicas, Universidade Federal do Rio de Janeiro (UFRJ), Rio de Janeiro, Brazil*

ABSTRACT

In the present paper we aimed to characterize epigenetic aspects and analyze *TP53* transcription in the 21 T series, composed of breast cell lines: non-cancerous H16N2; Atypical Ductal Hyperplasia 21PT; Ductal Carcinoma in situ 21NT and Invasive Metastatic Carcinoma 21MT1. We detected a global genomic hypomethylation in 21NT and 21MT1. The histone modification markers analysis showed an important global decrease of the active chromatin mark H4Ac in 21MT1 relative to the other cell lines while the repressive mark H3K9Me3 were not significantly altered. The mRNA levels of DNA methylation and histone modification key enzymes are consistent with the observed genomic hypomethylation and histone hypoacetylation. The expression of DNMT3A/B increased at the initial stages of oncogenesis and the expression of DNMT1 and HAT1 decreased at the advanced stages of breast cancer. Using a confocal immunofluorescent assay, we observed that H4Ac was mostly located at the periphery and the repressive mark H3K9Me3, at the center of 21NT and 21MT1 cells nuclei. *TP53* P1 promoter was found to be in an open chromatin state, with a relatively high enrichment of H4Ac and similar *TP53* transcription levels in all 21 T cell lines. In conclusion, we observed epigenetic alterations (global genome hypomethylation, global hypoacetylation and accumulation of pericentric heterochromatin) in metastatic breast cancer cells of the 21 T series. These alterations may act at later stages of breast cancer progression and may not affect *TP53* transcription at the P1 promoter. J. Cell. Biochem. 116: 533–541, 2015.

KEY WORDS: EPIGENETICS; BREAST CANCER PROGRESSION; 21T CELL LINES; DNA METHYLATION; HISTONE ACETYLATION; *TP53*

Breast cancer is the most frequent cancer among women and ranks among the top five cancer killers, according to the World Health Organization (http://www.who.int/mediacentre/factsheeets/fs297/en; 2013). Inherited and acquired mutations in genetic material as well as epigenetic modifications contribute to breast cancer progression and development [Albert and Helin, 2010; Stefansson and Esteller, 2013]. DNA methylation is one of the most studied types of epigenetic modification; it is generally implicated in gene silencing [Jones, 2012]. DNA methyltransferases (DNMTs) constitute a family of enzymes involved in DNA methylation and its members, DNMT1, 2, 3A and 3B, cooperate to maintain the methylation status of the genomic DNA or introduce de novo methyl groups [Denis et al., 2011]. Modification of histones, leading to chromatin changes, is also a relevant aspect of the epigenetic control of gene expression, example, activation or repression of genes involved in DNA repair, cell cycle, and cancer progression [Albert and Helin 2010; Akhavan-Niaki and Samadani, 2013; Badeaux and Shi, 2013]. Histone acetyl-transferases (HATs) catalyze reversible acetylation of histones which are linked to open chromatin and gene activation. HAT1 (KAT1) is the founding member of a super-family of HATs and is responsible for acetylation of histone H4 (H4Ac), a marker of transcriptionally active chromatin

Conflicts of interest: None declared.

Grant sponsor: FAPERJ-Brazil; Grant sponsor: CAPES-COFECUB; Grant sponsor: Universidade do Estado do Rio de Janeiro.

*Correspondence to: Claudia V. de Moura Gallo, Laboratório de Biologia Molecular de Tumores (LBMT), Universidade do Estado do Rio de Janeiro (UERJ), Pavilhão Haroldo Lisboa da Cunha, sala 525/6 Rua São Francisco Xavier, 524, Rio de Janeiro, RJ, Brasil. E-mail: cgallo8@yahoo.com

Manuscript Received: 26 March 2014; Manuscript Accepted: 24 October 2014

Accepted manuscript online in Wiley Online Library (wileyonlinelibrary.com): 30 October 2014

DOI 10.1002/jcb.25003 • © 2014 Wiley Periodicals, Inc.

or euchromatin [Luo et al., 2011; Yuan and Marmorstein, 2013]. Inversely, histone deacetylases (HDACs) control histone deacetylation levels and make histones more permissive to other modifications [Di Cerbo and Schneider, 2013]. Histone methyl-transferases (HMTs) catalyze reversible methylation of histones and can be linked to open or closed chromatin regions [Greer and Shi, 2012]. One of the HMTs, SUV39H1, is responsible for tri-methylation of histone H3 lysine 9 (H3K9me3), a strong marker of constitutive, transcriptionally inactive heterochromatin [Rice et al., 2003]. Decreased global DNA methylation and increased methylation of some crucial control gene promoters are important features of cancer cells [Park et al., 2011; Hon et al., 2012; Akhavan-Niaki and Samadani, 2013]. Chromatin remodeling was also observed during carcinogenesis [Locke and Clark, 2012]. Understanding how these mechanisms act is very important and cell models of cancer progression help this task. In breast cancer, several cell models are used to analyze the malignant transformation [Kern et al., 1994; Ethier, 1996; Chakrabarti et al., 2012]. A suitable and well characterized series of breast cells at different stages, known as 21 T series of cell lines, was developed in the 90's [Band et al., 1990; Liu et al., 1994]. It is composed of four cell lines isolated from the same patient: H16N2, representative of adjacent non-tumoral breast cells; 21PT, representative of Atypical Ductal Hyperplasia (ADH) cells; 21NT of Ductal Carcinoma In Situ (DCIS), and 21MT1 of Invasive Metastatic Carcinoma (IMC) [Souter et al., 2010]. A significant increase in migration levels and colony formation capability was described in H16N2 to 21MT1 cells [Qiao et al., 2007]. This is an exceptional model to study breast cancer progression, including epigenetic alterations; however, the epigenetic changes occurring in this model of tumor progression remain unknown. In the present paper we have characterized epigenetic changes in the 21 T series and determined transcriptional levels of the tumor suppressor gene *TP53*. P53 is a master transcription factor intrinsically involved in cancer development. Although its expression at protein level is well described, the regulation of its transcription during cancer progression is not well known. Here we found clear epigenetic alterations in the metastatic cells 21MT1 and open chromatin state of *TP53* P1 promoter with similar levels of *TP53* transcription in all 21 T cell lines.

RESULTS

GLOBAL GENOME HYPOMETHYLATION IN METASTATIC 21MT1 CELLS

Genome hypomethylation is one of the features of malignant cells [Hon et al., 2012]. Therefore, to characterize the DNA methylation profile of each cell line of the 21 T series, we determined their relative global genomic methylation. The genomic DNA isolated from these cell lines was separated in two parts. One part was digested with a methylation sensitive *HpaII* restriction endonuclease, another with a methylation insensitive *MspI*. The digested DNA was run on agarose gels, and the intensities of *HpaII*- and *MspI*-digested DNA, relative to intact genomic DNAs, were compared using Image J® software. The percentage of relative global genomic methylation was calculated using the following formula: (HpaII-MspI) × 100/genomic DNA. The non-cancerous H16N2 and the hyperplasic 21PT had 29.52 and 36.23% of relative global genome methylation, respectively, while cancerous 21NT and the metastatic 21MT1 had lower global methylation levels, 15.03 and 15.32%, respectively. Therefore, we could observe a small increase in global genomic methylation going from H16N2 to the hyperplasic 21PT, although not statistically significant, and a statistically significant decrease from H16N2 to the cancerous 21NT and metastatic 21MT1 cell lines (Fig. 1).

GLOBAL DECREASE OF ACTIVE CHROMATIN MARKER H4Ac IN METASTATIC 21MT1 CELLS

To study chromatin remodeling during the progression to breast cancer, we determined global expression of markers of chromatin organization, H4Ac, hallmark of active chromatin and H3K9Me3, hallmark of repressive chromatin using Western-blot analysis. Whole-cells proteins were extracted from the 21 T cell lines, separated by 15% SDS-PAGE, and incubated with anti-H4Ac, anti-H3K9me3 antibodies as well as with anti-totalH3 (loading control). Relative abundance of these markers was calculated relative to anti-totalH3. Figure 2 shows a progressive decrease in total H4Ac observed between the non-cancerous H16N2 and the cancer cell lines. The metastatic 21MT1 had the lowest level of H4Ac. The global levels of H3K9Me3 increased from the non-cancerous to cancer cells although the difference was not statistically different among the 21 T series cell lines.

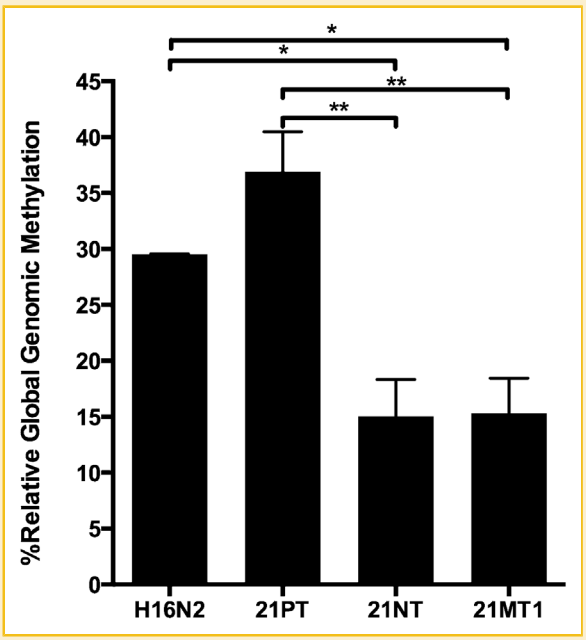

Fig. 1. Relative global genomic methylation levels of the 21 T cell lines. Relative global genomic methylation of the non-cancerous cells (H16N2), atypical ductal hyperplasia stage (21PT), ductal in situ (21NT), and metastatic carcinoma (21MT1). The global genomic methylation was estimated by *HpaII* and *MspI* restriction endonucleases as described in Materials and Methods. Error bars represent S.E.M. of four different experiments; *t*-test: $^{*}P < 0.05$; $^{**}P < 0.005$.

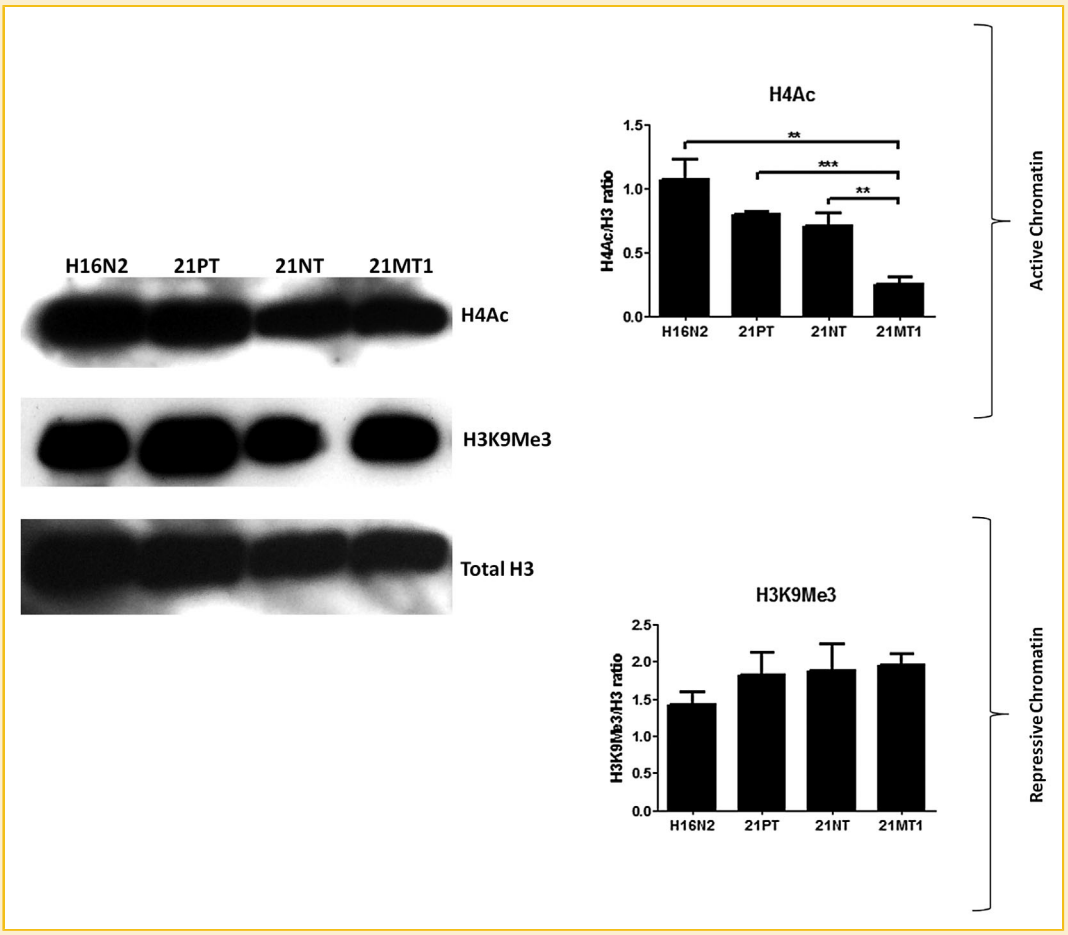

Fig. 2. Expression of chromatin markers H4Ac and H3K9Me3 in 21 T cell lines. Western Blot analysis of active histone marks H4Ac and the repressive mark H3K9Me3 in non-cancerous (H16N2), atypical ductal hyperplasia (21PT), ductal in situ carcinoma (21NT), metastatic carcinoma (21MT1) cell lines. Total H3 expression was used as control. All charts represent the ratio between histone marks and total H3 histone, by densitometry in Image J® software. Statistical test: one-way ANOVA with Bonferroni post-test. *$P < 0{,}05$; **$P < 0{,}005$.

DIFFERENT EXPRESSION OF KEY GENES LINKED TO EPIGENETIC MODIFICATIONS IN THE 21 T CELL LINES

We have next used RT-qPCR to analyze mRNA levels of enzymes linked to the epigenetic modifications observed during breast cancer progression, DNMT1, DNMT3A/B, SUV39H1, and HAT1, in the 21 T cell series (Table I, Suppl. Table 1 and Suppl. Fig. 1). From non-cancerous H16N2 to hyperplasic 21PT, the mRNA levels of the analyzed enzymes were up-regulated, with the exception of DNMT1 which was strongly down-regulated ($P = 0.0416$). In contrast to the initial step of breast cancer progression, DNMT1 was up-regulated ($P = 0.0103$) in non-cancerous 21PT as compared to the 21NT cells, but DNMT3B was down-regulated ($P = 0.0011$). Finally, the 21NT to metastatic 21MT1, DNMT1, DNMT3A, and HAT1 were down-regulated ($P = 0.0103$, $P = 0.0060$, and $P = 0.0087$, respectively). Thus, high levels of genomic methylation at non-cancerous cells (H16N2) may be

TABLE I. Expression of Key Genes Responsible for Epigenetic Modifications in 21 T Series Cell Lines

Genes	H16N2	21PT	21NT	21MT1
DNMT1	0.045552300	0.004120244	0.0389197100	0.0033738800
DNMT3A	0.000246858	0.003024751	0.0013899000	0.0001814570
DNMT3B	0.000175841	0.008179488	0.0000875218	0.0002220440
SUV39H1	0.000002911	0.000367855	0.0008094410	0.0001528890
HAT1	0.000245947	0.029841590	0.0448822600	0.0000071696

Values correspond to fold change by RT-qPCR analysis relative to β-actin gene.

related to an increase of DNMT1 mRNA expression while a decrease in global DNA methylation and global histone H4 acetylation during invasive metastatic cancer progression may be linked to a decrease in DNMT1 and HAT1 mRNA levels.

ACCUMULATION OF PERICENTRIC HETEROCHROMATIN IN THE METASTATIC 21MT1 CELLS

Having determined the expression of the global histone modification marks H4Ac and H3K9Me3 in the 21 T series cell lines, we have next investigated the nuclear distribution of these markers during breast cancer progression using confocal immunofluorescence. Briefly, fixed cells on round cover-slips, were blocked in 3% PBS/BSA, incubated with anti-H4Ac and anti-H3K9me3 primary antibodies and incubated with secondary antibodies conjugated with Alexa Fluor 488 and 555 for H3K9Me3 and H4Ac, respectively. Nuclei were stained with DAPI. From 110 to 400 nuclei in 30 fields were analyzed by confocal microscopy. Distribution of histone marks in the nuclei was detected by plotting fluorescence intensity using Leica Application Suite Advanced Fluorescence Lite 2.4.1® software. The obtained results are presented in Figure 3A–C. For a more accurate analysis of nuclear distribution, peripheral or pericentral, of histone marks, we calculated the ratio of fluorescence intensity in the central part of the nuclei areas, relative to fluorescence intensity in the peripheral areas using ImageJ® software (Fig. 3C, Supplementary Table 2). A ratio of >1 indicates enrichment toward the center of the nucleus, and a ratio of <1 indicates a peripheral distribution. We observed that the H4Ac marker was mostly located in the nuclear periphery in all cell lines (a ratio of 0.52–0.83), although it was less central in aggressive tumour cells (Fig. 2). H3K9me3 was differently distributed among the cell lines, being progressively more central in the 21NT and 21MT1 nuclei (a ratio of 1.30 and 1.62, respectively). Hence, we have observed a redistribution of H3K9me3 towards the center of the nuclei during cancer progression.

HOMOGENEOUS *TP53* TRANSCRIPTION AND OPEN CHROMATIN STATE OF *TP53* P1 PROMOTER IN 21 T CELL LINES

To check the possible influence of the observed chromatin alterations during breast cancer progression on gene regulation, we next analyzed the chromatin state of the *TP53* P1 promoter and transcription of the master regulator gene *TP53* in the 21 T cell lines. We have used ChIP followed by qPCR to analyze chromatin markers H4Ac (fold enrichment relative to the active β-actin gene region) and H3K9Me3 (fold enrichment relative to the repressed alpha-satellite region) at the *TP53* promoter 1. The promoter was enriched in H4Ac indicating an open local chromatin organization, permissive to *TP53* transcription in all 21 T cell lines. A low abundance of H3K9me3 at the *TP53* P1 promoter (Fig. 4A) is in agreement with the *TP53* transcription data. We have next used RT-qPCR to quantify *TP53* mRNA levels in these cells. The *TP53* transcriptional levels were not statistically different among the cell

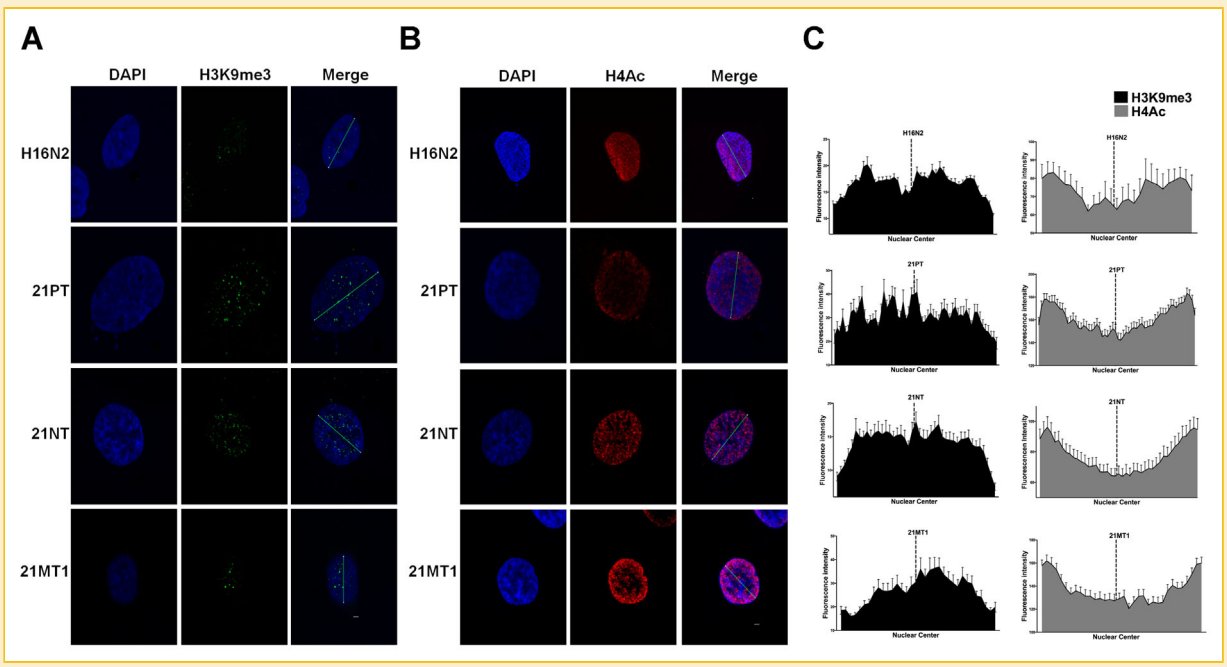

Fig. 3. Nuclear distribution of chromatin markers H4Ac and H3K9me3 in 21 T cell lines. Representative confocal nuclear cell images for each 21 T cell line: (A) H3K9me3 (green), (B) H4Ac (red). (C) H3K9me3 (dark) and H4Ac (gray) fluorescence intensity distribution. Each abscissa point represents a single pixel of a diametral nuclear ROI, the bold grid line indicates the nuclear center position and the ordinate represents the fluorescence intensity in arbitrary units. For graphic markers distribution, confocal image analysis was evaluated by fluorescent intensity pixels of the markers H3K9me3 and H4Ac, in a diametral nuclear ROI, for 110–400 nuclei (30 fields) for each 21 T cell line. Each error bar represents S.E.M. of fluorescent intensity pixels for all analyzed nuclei, experimental triplicates Scale bar = 2 μM.

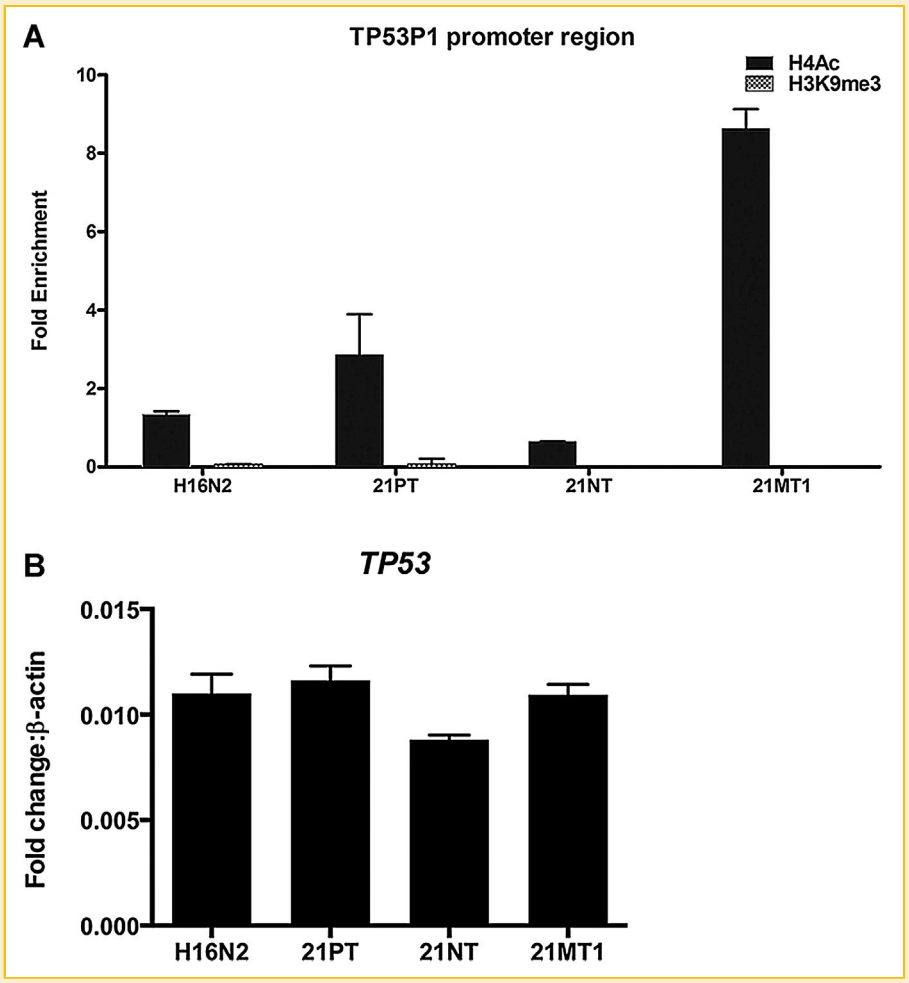

Fig. 4. Chromatin state of the *TP53* P1 promoter and *TP53* transcription levels in 21 T cell lines. ChIP assay of *TP53* promoter P1 in (A) tumor progression (21T series). (B) Relative *TP53* transcription levels measured by RT-qPCR in 21 T series. Error bars represent S.E.M. of three independent experiments.

lines of the 21 T series, in agreement with the H4Ac ChIP data (Fig. 4B).

DISCUSSION

Breast cancer is a heterogeneous disease and one of the most common aggressive cancers in women. Despite intensive research efforts, the causes of breast cancer development and aggressiveness are far from being revealed. Recently, alterations in the cell genome and epigenome were found to contribute to cancer progression [Baylin and Jones, 2011; Locke and Clark, 2012; Schweiger et al., 2013].

Breast cancer cell lines have been established to help understand breast cancer development in vitro, with a relatively good correlation with the disease in vivo [Perou et al., 2000; Neve et al., 2006; Vargo-Gogola and Rosen, 2007]. The 21 T series, comprising the H16N2, 21PT, 21NT, 21MT1 cell lines was isolated from successive biopsies from the same patient. This cell series represents the progression of a human breast cancer in three stages: (1) from adjacent Non-cancerous (N) to Atypical Ductal Hyperplasia (ADH); (2) from ADH to Ductal Carcinoma in situ (DCIS); and (3) from DCIS to Invasive Metastatic Carcinoma (IMC). Except for H16N2, 21T cells are HER-2 positive and do not express p53 protein, because of a gene mutation c.96_97ins1 [Band et al., 1990; Band and Sager, 1991; Liu et al., 1994].

In the present paper we aimed to characterize the epigenetic aspects of the 21 T series and also study whether the observed molecular alterations could influence the transcription of the key tumor suppressor gene *TP53*. We then performed analysis of global genomic DNA methylation; mRNA expression of key enzymes of DNA methylation (DNMT1, DNMT3A/3B) and histone modification (SUV39H1 and HAT1); expression of active (H4Ac) and repressive (H3K9Me3) chromatin markers, as well as their nuclear distribution. We will discuss below our results in the light of the different stages of breast cancer progression.

From the non-cancerous H16N2 to ADH 21PT, the global genomic methylation did not statistically change, remaining at high levels. The transcription of the DNA methylation enzymes DNMT1 and DNMT3A/B was down and up-regulated, respectively. These results

suggest that higher levels of global genomic methylation at the initial stage of breast cancer progression are maintained by DNMT3A/B rather than DNMT1, as their mRNA levels are approximately 11 fold up- and down-regulated, respectively. In agreement with our data, higher levels of methylation in CpG islands were found at initial stages of breast cancer progression [Park et al., 2011; Locke and Clark, 2012].

From ADH 21PT to DCIS 21NT cells, a highly significant decrease of global methylation was detected. However, DNMT1 and DNMT3B were oppositely regulated with an increase and a decrease in their mRNA levels, respectively. As observed at the previous stage, we could not detect significant alterations in global expression of histone epigenetic modification marks, but the repressive marker H3K9me3 was more concentrated in the center of the cell nuclei in DCIS. This is the first report of heterochromatic changes through loss of peripheral and gain of pericentric heterochromatin, from hyperplasic to cancerous non-metastatic breast cells. Earlier reports described a pericentric heterochromatin accumulation from non-cancerous to metastatic breast cells [Carone and Lawrence, 2013].

From DCIS 21NT to IMC 21MT1 cells, the global genomic methylation was not altered and we detected an important decrease of *DNMT1*, *DNMT3A*, and *HAT1* mRNA levels as well as a global decrease of H4Ac expression with a high concentration of repressive/heterochromatin marker H3K9me3 in pericentric regions, in agreement with the published data [Carone and Lawrence, 2013]. Global genomic hypomethylation and higher levels of H3K9me3 have been associated with malignant metastatic transformation in melanocytes. In addition, lower DNMT1 transcription levels were found exclusively in non-cancerous melanocytes and higher DNMT3A transcription levels only in metastatic melanoma [Molognoni et al., 2011]. The inverse correlation of transcription levels between DNMT1 and DNMT3A/B that we have observed in normal versus cancerous non-metastatic breast cell lines, could suggest a compensatory role of these enzymes in breast cancer progression. The global hypoacetylation of histone H4 is likely linked to low transcription levels of HAT1 observed in the 21MT1 metastatic breast cell line. This could silence or reduce the expression levels of tumor suppressor genes [Di Cerbo and Schneider, 2013] and lead to deficient homologous recombination repair [Yang et al., 2013].

Having studied the global changes in chromatin organization, we decided to analyze the expression level of the master tumor suppressor gene *TP53,* as well as the chromatin organization of *TP53* gene P1 promoter region in 21T cell lines. We did not find any significant differences in *TP53* expression among the cell lines. *TP53* P1 promoter was enriched in H4Ac, with H3K9me3 significantly depleted, characterizing an open chromatin conformation. The maintenance of an open chromatin status in the promoter region P1 as well as the homogeneous expression of *TP53* gene through breast cancer progression, reinforces that the protein p53 may be preferentially regulated by post-translational modifications [Dehart et al., 2013]. Of note, the cancerous cells of the 21T series present p53 protein loss due to a frame-shift mutation [Liu et al., 1994].

Our results reinforce the link between key epigenetic alterations, such as global genomic hypomethylation, global hypoacetylation, and accumulation of pericentric heterochromatin in metastatic breast cancer, as described elsewhere [Suzuki et al., 2009; Locke and Clark, 2012; Carone and Lawrence, 2013; Di Cerbo and Schneider, 2013]. In addition, based in our results, we suggest that these key epigenetic phenotypes manifest at later stages of metastatic breast cancer progression. The epigenetic modifications we have observed during breast cancer progression based on the 21T series, could be essential to change the 'epigenetic state' of differentiated cells into a less differentiated and more aggressive state typical of metastatic cells [Halley-Stott and Gurdon, 2013].

METHODS

CELL CULTURE

The 21T cell series (21PT, 21NT, and 21MT1) were kindly provided by Dr. Pierre Hainaut (International Agency for Research on Cancer; Lyon, France) and the H16N2 by Dr. Vimla Band (Department of Genetics, Cell Biology and Anatomy; University of Nebraska Medical Center). Cells were cultured in α-MEM medium (#12–169F, Lonza®) supplemented with l-glutamine 4 mM (Gibco®), 10% fetal bovine serum (Gibco®), 10 ug/ml insulin (Sigma®), 0.5 ug/ml hydrocortisone (Sigma®), 20 ng/ml EGF (Sigma®), 1X anti-anti (antibiotic-antimycotic, Gibco®), and 10 ug/ml ciprofloxacin at 37 °C in a humidified atmosphere at 5% CO_2. Cells counting and viability were carried out on Moxi Z Mini (Orflo®). All the 21T cell lines were genotyped to confirm their allelic profile. Cultures were routinely checked for mycoplasma contamination.

DETERMINATION OF THE GLOBAL METHYLATION LEVELS BY DIGESTION OF GENOMIC DNA WITH RESTRICTION ENZYMES *MsPL* AND *HpaII*

Genomic DNA from 21T series cells was extracted and purified using Invisorb Spin Tissue Kit (Invitek®) and quantified using NanoDrop 2000 (Thermo Scientific®). Three microgram of DNA was digested with 30 units of either a methylation sensitive *HpaI* restriction endonuclease, or with a methylation insensitive *MspII* (New England Biolabs®) for 16 h at 37 °C, followed by addition of 30 units more for 1 h and heat inactivation for 20 min at 65 °C. The samples were run in 1% agarose gels and stained with ethidium bromide (Suppl. Fig. 2). The percentage of relative global genomic methylation was measured by comparing band intensities of digested and intact genomic DNA using ImageJ software and then calculated using the following formula: (HpaII - MspI) × 100/genomic DNA, as described elsewhere [Molognoni et al., 2011].

WESTERN BLOT

Cells were washed twice with ice-cold 1X PBS and lysed with a buffer containing 150 mM NaCl, 1 mM EDTA, 50 mM Tris-HCl (pH 7.5), 0.5% NP-40, and a protease inhibitor cocktail (Roche). Samples were incubated on ice for 30 min. Protein extracts (10 μg) were heat denatured and separated by SDS-PAGE. Proteins were transferred to a nitrocellulose membrane (BioRad®), blocked for 1 h with 5% non-fat dry milk in TBST (136 mM NaCl, 2.6 mM KCl, 24 mM Tris-HCl pH 7.4, and 0,1% Tween 20) and incubated for 1 h with the following primary human antibodies diluted 1:4000 in TBST: H4 pan-acetyl (#39243, Active Motif®), tri-methyl H3K4 (#07–473, Millipore®),

tri-methyl H3K9 (#05–1242, Millipore®), tri-methyl H3K27 (#17–622, Millipore®), and total H3 (#4620, Cell Signalling®). The band signals were visualized by chemoluminescence using the Immobilion Western kit (#WBKLS0500, Millipore®) after incubation with secondary horseradish-peroxidase conjugated antibodies (KPL®), and quantitated by ImageJ® software.

mRNA EXPRESSION ANALYSIS

Total RNA was isolated using Trizol (Life Technologies®). cDNA synthesis and real-time PCR analysis with gene-specific primers were carried out using the GoTaq 2-Step RT-qPCR System (Promega®) according to the manufacturer's instruction. RT-qPCR was carried out on the 7,500 Real-time PCR system (Applied Biosystems®). The RNA quality was assessed by 260/280 nm absorbance ratio of 1.8–2.1 in Nanodrop ND-2000 (Thermo®). Also, all the reverse transcriptase reactions were done with a negative control without enzyme. This same negative control was used in all qPCR reactions, without any amplification. The housekeeping β-*actin* gene was used as the internal control and PCR products were measured by SYBR Green method with ΔΔCT. The primers (Eurofins MWG Operon®) used were as follows (F-Forward; R-Reverse):

DNMT1—F: CCTTGGAGAACGGTGCTCAT/R: CTTAGCCTCTCCATC-GACT
DNMT3A—F: AGAAGTGTACACGGACATGTGG/R: AGGAGATGCA-GATGTCCTCAAT
DNMT3B—F: CATCAAAGTTTCTGCTGCTCAC/R: CAAAGATCCTTT-CGAGCTCAGT
SUV39H1—F: ATGGAGTACGTGGGAGAGATCA/R: TCTTGTGGCA-AAGAAAGCGATG
HAT1—F: CGTGGATGATGAAAGATGGCAC/R: TTTTGGATGGATC-TTCCGCTGT.

IMMUNOFLUORESCENCE, CONFOCAL MICROSCOPY, AND IMAGE ANALYSIS

Cells were grown on round coverslips inside a 24-well test plate, then they were fixed in a 4% paraformaldehyde solution for 10 min, rinsed with PBS 1X, and permeabilized with 0,5% Triton X-100 for 10 min. They were then washed three times with PBS 1X, followed by 30 min of incubation with 5 mM Ammonium Chloride. Cells were rinsed with 1% PBS/BSA solution and incubated in 3% PBS/BSA solution for 30 min. After fixation, the cells were incubated with the primary antibodies diluted 1:200 in 1% PBS/BSA (anti-H3K9me3 and anti-H4Ac, the same used for Western Blot) for 16 h, rinsed with 1% PBS/BSA, blocked for 30 min in 3% PBS/BSA and then were incubated with the secondary antibodies (Alexa Fluor 488 #A21202 for H3K9Me3 and Alexa Fluor 555 #A31572 for H4Ac) for 2 h in the dark. After that, cells were washed with 1% PBS/BSA and 1X PBS; and incubated with DAPI (1:3000 in 1%PBS/BSA) for 5 min in the dark. After washing with PBS 1X, the coverslips were inverted onto glass slides with mounting medium (SlowFade-Antifade kit, Invitrogen®) and were analyzed under Leica® TCS SP5 AOBS confocal laser microscope equipped with a 63X oil immersion objective. Data acquisition was made in triplicate in three different experiments, with 30 fields for each slide by counting 110–400 nuclei per each cell line. Distribution of nuclear markers was analyzed by plotting the means of each pixel in a diametral ROI designed for each nucleus, with Leica Application Suite Advanced Fluorescence Lite 2.4.1® software. Each graphic point corresponds to fluorescence intensity of a single pixel. All fields were analyzed with Leica Application Suite Advanced Fluorescence Lite 2.4.1® software.

ChIP ASSAY

A total of 25×10^6 cells were cross-linked with 1% formaldehyde for 10 min in a rocking platform at room temperature. Cross-linking reaction was stopped with Glycine 0.125 M diluted in 1X PBS. The cells were washed with ice-cold 1X PBS and resuspended in 1 ml Lysis/Sonication cold buffer (1% SDS, 10 mM EDTA, and 50 mM Tris-HCl pH 7.5) with fresh 0.5 mM PMSF and 1X PIC (Protease Inhibitor Cocktail) and incubated for 30 min on ice. The lysates were homogenized with 10 strokes, centrifuged at 750*xg* for 5 min at 4 °C and the supernatant was discarded. The pellet was resuspended in 350 μL of Lysis/Sonication cold buffer with freshly added 1 mM PMSF and 1X PIC, sonicated on ice and centrifuged for 10 min with 2,000*xg* at 4 °C. The supernatant contains the extracted chromatin. Immunoprecipitation was carried out overnight at 4 °C with constant agitation in an immunoprecipitation buffer (5 mM Tris-HCl pH 8.0, 15 mM NaCl, 1 mM EDTA, and 0.1% NP40) with 20 μg of chromatin, 750 μg of Protein G dynabeads #100.03D (Invitrogen®), 4 μg of antibodies H4 pan-acetyl (#39243, Active Motif®), tri-methyl H3K9 (#05–1242, Millipore®), normal rabbit IgG (#PP64B, Millipore®; control), and 1X PIC. All the immunoprecipitations were made with at 1:4 dilutions. The magnetic beads were washed six times with the immunoprecipitation buffer and the chromatin was eluted with the Lysis/sonication buffer for 15 min at room temperature with constant agitation. The magnetic beads were separated from eluted chromatin and the proteinase K digestion and reverse cross-link were done as described above. DNA was cleaned-up by the standard Phenol-Chloroform method and submitted to qPCR.

qPCR was carried out using the standard Syber-Green method with the Mastermix (Roche®). All fold enrichment values of H4Ac and H3K9me3 are relative to the fold enrichment values of the β-actin gene region or the alpha-satellite region, respectively. All primers, synthesized by SIGMA®, are listed in 5–3′ and F-forward/R-reverse:

TP53P1 F—GCGTGTCACCGTCGTGGAAAG/R—GGAGCCTCGCAGG-GGTTGATG
β-actin gene region F—GACGTAGCACAGCTTCTCCT/R—GGGACC-TGACTGACTACCTCAT
Alpha-Satellite (#CS207313, Millipore®) F—CTGCACTACCTGAA-GAGGAC/R— GATGGTTCAACACTCTTACA.

All chromatin extraction, immunoprecipitation, and qPCR were done in triplicate and the error bars correspond to the S.E.M. of three different experiments.

STATISTICAL ANALYSIS

The statistical analysis was carried out using the Graphpad® software 6.0, with 95% of CI, using non-parametric *t*-test. All error bars represent S.E.M. (standard error of the mean).

ACKNOWLEDGMENTS

We thank Dr. Pierre Hainaut and Dr. Vilma Band for the gift of cell lines. The research in YV lab was funded by grants from Fondation de France, Institute National de Cancer (INCa), and CAPES-COFECUB. The research was funded by grants of FAPERJ-Brazil, CAPES-COFECUB, and Universidade do Estado do Rio de Janeiro.

AUTHORS' CONTRIBUTIONS

SGC-Jr carried out all the experiments, result analysis, including immunoflorescence confocal microscopy image analysis, and drafted the manuscript. APAS carried out cell cultures and immunofluorescence confocal microscopy. GMV participated in the immunofluorescence confocal microscopy. LF participated in the DNA global methylation assays and mRNA expression assays. YV participated in the study design and critical revision of manuscript. CVMG conceived the study, participated in its design and coordination, and wrote the manuscript. All authors read and approved the final manuscript.

REFERENCES

Akhavan-Niaki H, Samadani AA. 2013. DNA methylation and cancer development: Molecular mechanism. Cell Biochem Biophys 67(2):501–513.

Albert M, Helin K. 2010. Histone methyltransferases in cancer. Sem Cell Dev Biol 21(2):209–220.

Badeaux AI, Shi Y. 2013. Emerging roles for chromatin as a signal integration and storage platform. Nature reviews. Mol Cell Biol 14(4):211–224.

Band V, Sager R. 1991. Neoplastic transformation in human cell culture. In: Rhim JS, Dritschilo A, editors. Neoplastic transformation in human cell culture. Totowa, NJ: Humana Press. pp 169–178.

Band V, Zajchowski D, Swisshelm K, Trask D, Kulesa V, Cohen C, Connolly J, Sager R. 1990. Tumor progression in four mammary epithelial cell lines derived from the same patient tumor progression in four mammary epithelial cell lines derived from the same patient. Cancer Res 50:7351–7357.

Baylin SB, Jones PA. 2011. A decade of exploring the cancer epigenome - biological and translational implications. Nature reviews. Cancer 11(10): 726–734.

Carone DM, Lawrence JB. 2013. Heterochromatin instability in cancer: From the Barr body to satellites and the nuclear periphery. Sem Cancer Biol 23(2): 99–108.

Chakrabarti A, Verbridge S, Stroock AD, Fischbach C, Varner JD. 2012. Multiscale models of breast cancer progression. Ann Biomed Eng 40(11): 2488–2500.

Dehart CJ, Chahal JS, Flint SJ, Perlman DH. 2013. Extensive post-translational modification of active and inactivated forms of endogenous p53. Mol Cell Proteomics: MCP, p.M113.030254–.

Denis H, Ndlovu MN, Fuks F. 2011. Regulation of mammalian DNA methyltransferases: A route to new mechanisms. EMBO Reports 12(7):647–656.

Di Cerbo V, Schneider R. 2013. Cancers with wrong HATs: The impact of acetylation. Briefings Function Genom 12(3):231–243.

Ethier SP. 1996. Human breast cancer cell lines as models of growth regulation and disease progression. J Mammary Gland Biol Neoplasia 1(1): 111–121.

Greer EL, Shi Y. 2012. Histone methylation: A dynamic mark in health, disease and inheritance. Nature reviews. Genetics 13(5):343–357.

Halley-Stott RP, Gurdon JB. 2013. Epigenetic memory in the context of nuclear reprogramming and cancer. Briefings Function Genom 12(3):164–173.

Hon GC, Hawkins RD, Caballero OL, Lo C, Lister R, Pelizzola M, Valsesia A, Ye Z, Kuan S, Edsall LE, Camargo AA, Stevenson BJ, Ecker JR, Bafna V, Strausberg RL, Simpson AJ, Ren B. 2012. Global DNA hypomethylation coupled to repressive chromatin domain formation and gene silencing in breast cancer. Genome Res 22(2):246–258.

Jones P. 2012. Functions of DNA methylation: Islands, start sites, gene bodies and beyond. Nature reviews. Genetics 13(7):484–492.

Kern FG, McLeskey SW, Zhang L, Kurebayashi J, Liu Y, Ding IY, Kharbanda S, Chen D, Miller D, Cullen K. 1994. Transfected MCF-7 cells as a model for breast-cancer progression. Breast Cancer Res Treatment 31(2–3):153–165.

Liu XL, Band H, Gao Q, Wazer DE, Chu Q, Band V. 1994. Tumor cell-specific loss of p53 protein in a unique in vitro model of human breast tumor progression. Carcinogenesis 15(9):1969–1973.

Locke WJ, Clark SJ. 2012. Epigenome remodelling in breast cancer: Insights from an early in vitro model of carcinogenesis. Breast Cancer Res: BCR 14(6):215.

Luo X, Guo S, Guo Y, Zhang C. 2011. Breast cancer – focusing tumor microenvironment, stem cells and metastasis. Breast Cancer – Focus Tumor Microenviron Stem Cells Metastasis 15:321–342. doi: 10.5772/1747.

Molognoni F, Cruz AT, Meliso FM, Morais AS, Souza CF, Xander P, Bischof JM, Costa FF, Soares MB, Liang G, Jones P a., Jasiulionis MG. 2011. Epigenetic reprogramming as a key contributor to melanocyte malignant transformation. Epigenetics 6(4):450–464.

Neve RM, Chin K, Fridlyand J, Yeh J, Baehner FL, Fevr T, Clark L, Bayani N, Coppe J-P, Tong F, Speed T, Spellman PT, DeVries S, Lapuk A, Wang NJ, Kuo W-L, Stilwell JL, Pinkel D, Albertson DG, Waldman FM, McCormick F, Dickson RB, Johnson MD, Lippman M, Ethier S, Gazdar A, Gray JW. 2006. A collection of breast cancer cell lines for the study of functionally distinct cancer subtypes. Cancer Cell 10(6):515–527.

Park SY, Kwon HJ, Lee HE, Ryu HS, Kim S-W, Kim JH, Kim IA, Jung N, Cho N-Y, Kang GH. 2011. Promoter CpG island hypermethylation during breast cancer progression. Virchows Archiv: An International J Pathol 458(1): 73–84.

Perou CM, Sørlie T, Eisen MB, van de Rijn M, Jeffrey SS, Rees CA, Pollack JR, Ross DT, Johnsen H, Akslen LA, Fluge O, Pergamenschikov A, Williams C, Zhu SX, Lønning PE, Børresen-Dale AL, Brown PO, Botstein D. 2000. Molecular portraits of human breast tumours. Nature 406(6797): 747–752.

Qiao M, Iglehart JD, Pardee AB. 2007. Metastatic potential of 21 T human breast cancer cells depends on Akt/protein kinase B activation. Cancer Res 67(11):5293–5299.

Rice JC, Briggs SD, Ueberheide B, Barber CM, Shabanowitz J, Hunt DF, Shinkai Y, Allis CD. 2003. Histone methyltransferases direct different degrees of methylation to define distinct chromatin domains. Mol Cell 12(6):1591–1598.

Schweiger M-R, Barmeyer C, Timmermann B. 2013. Genomics and epigenomics: New promises of personalized medicine for cancer patients. Brief Funct Genomics 12(5):411–421.

Souter LH, Andrews JD, Zhang G, Cook AC, Postenka CO, Al-Katib W, Leong HS, Rodenhiser DI, Chambers AF, Tuck A. 2010. Human 21 T breast epithelial cell lines mimic breast cancer progression in vivo and in vitro and show stage-specific gene expression patterns. Lab Invest; J Tech Methods Pathol 90(8):1247–1258.

Stefansson O, Esteller M. 2013. Epigenetic modifications in breast cancer and their role in personalized medicine. Am J Pathol 183(4):1–12.

Suzuki J, Chen Y-Y, Scott GK, Devries S, Chin K, Benz CC, Waldman FM, Hwang ES. 2009. Protein acetylation and histone deacetylase expression

associated with malignant breast cancer progression. Clin Cancer Res 15(9): 3163–3171.

Vargo-Gogola T, Rosen JM. 2007. Modelling breast cancer: One size does not fit all. Nature reviews. Cancer 7(9):659–672.

Yang X, Li L, Liang J, Shi L, Yang J, Yi X, Zhang D, Han X, Yu N, Shang Y. 2013. Histone acetyltransferase 1 promotes homologous recombination in DNA repair by facilitating histone turnover. J Biol Chem 288(25):18271–18282.

Yuan H, Marmorstein R. 2013. Histone acetyltransferases: Rising ancient counterparts to protein kinases. Biopolymers 99(2):98–111.

SUPPORTING INFORMATION

Additional supporting information may be found in the online version of this article at the publisher's web-site.